Int J Clin Exp Med 2016;9(8):16971-16980
www.ijcem.com /ISSN:1940-5901/IJCEM0032493

Original Article

Whole-brain voxel-based analysis of diffusion tensor imaging and its correlation with visual evoked potential in patients with optic neuritis

Kai Wu[1,2*], Xin Huang[1,3*], Gang Tan[2], Lei Ye[1], An-Hua Wu[2], Yu-Lin Zhong[1], Nan Jiang[1], Yi Shao[1]

[1]Department of Ophthalmology, The First Affiliated Hospital of Nanchang University, Nanchang 330006, Jiangxi, People's Republic of China; [2]Department of Ophthalmology, The First Affiliated Hospital of University of South China, Hengyang 421001, Hunan, People's Republic of China; [3]Department of Ophthalmology, The First People's Hospital of Jiujiang City, Jiujiang 332000, Jiangxi, People's Republic of China. [*]Equal contributors.

Received May 19, 2016; Accepted August 9, 2016; Epub August 15, 2016; Published August 30, 2016

Abstract: This study was to investigate the fractional anisotropy (FA) and mean diffusion (MD) values of diffusion tensor imaging (DTI) in the whole-brain voxel-based analysis of optic neuritis (ON) patients and examine their relationship with visual evoked potentials. A total of 12 (4 male, 8 female) patients with ON and 12 age-, sex-, and education-matched healthy controls (HCs) underwent magnetic resonance imaging (MRI). Imaging data were analyzed using two-sample *t*-tests to identify group differences in FA and MD values. Correlation analyses were performed to explore relationships between the FA and MD values of different brain regions and visual evoked potential (VEP) in subjects with ON. Compared with HCs, ON patients exhibited significantly decreased FA in the left cerebellum posterior lobe, left superior temporal gyrus, left extra-nuclear1, right middle frontal gyrus, and left middle frontal gyrus and increased FA in the right cerebellum_crus, right lentiform nucleus, bilateral anterior cingulum, left extra-nuclear2 and left precuneus. Meanwhile, increased MD was observed in the left inferior temporal gyrus, left superior temporal gyrus, left hippocampus, left anterior cingulate/caudate, right superior frontal gyrus, right precentral gyrus, and left inferior parietal lobule. VEP latency of the right eye in ON correlated positively with the FA values of the bilateral anterior cingulum (r = -0.583, P = 0.047) and negatively with the FA values of the left superior temporal gyrus (r = 0.653, P = 0.021). VEP amplitude of the right eye in ON subjects negatively correlated with the FA values of the left extra-nuclear2 (r = -0.592, P = 0.043). VEP latency of the left eye in ON correlated positively with the MD value of the left anterior cingulate/caudate (r = 0.707, P = 0.010) and negatively with MD values of the left inferior parietal lobule (r = 0.670, P = 0.017), while VEP amplitude of the left eye in ON showed negative correlation with MD values of the left inferior parietal lobule (r = -0.684, P = 0.014). These results suggest significant brain involvement in ON, which may reflect the underlying pathologic mechanism. Correlational results demonstrate that VEP in ON is closely associated with FA and MD in multiple brain regions.

Keywords: Optic neuritis, diffusion tensor imaging, fractional anisotropy, mean diffusion, visual evoked potential

Introduction

Optic neuritis (ON) is defined as inflammation of the optic nerve that leads to lesions of the optic nerve axons and retinal ganglion cell apoptosis. Patients with ON experience pain on eye movement in one eye and sudden vision loss; other symptoms include relative afferent pupillary defect (RAPD) and papillary edema. A previous survey reported an annual prevalence of 5 cases per 100,000 individuals in central Europe [1]. Optic neuritis is often the initial manifestation of multiple sclerosis (MS) [2]. The Optic Neuritis Treatment Trial (ONTT) described a patient with ON who showed significant improvements in color vision and contrast sensitivity within 6 months after corticosteroids treatment [3]. However, a subsequent study found no effect of corticosteroids on optic nerve atrophy [4].

Visual evoked potential (VEP) measurement is an important clinical test that has been studied in patients with ON. One study showed significantly prolonged multifocal (mf)VEP latency in subjects with ON, indicating a role for demyelin-

ation in axonal loss [5]. Notably, mfVEP amplitude reduction and latency delay have been observed after ON episodes [6]. In addition, VEP can be used to evaluate ON prognosis, and mfVEP amplitude improvement can contribute to functional recovery after acute ON [7].

Diffusion tensor imaging (DTI) is a widely used magnetic resonance imaging (MRI) modality that depicts water diffusion directionality as mean diffusivity (MD) and fractional anisotropy (FA) [8]. MD is a measure of the total amount of diffusion within a voxel and provides the overall magnitude of water diffusion. FA is a scalar value between zero and one and is calculated from the eigenvalues (λ1, λ2, λ3) of the diffusion tensor; it measures the overall directionality of water diffusion and reflects the complexity of cytoskeleton architecture, which restricts the intra- and extracellular water movement [9]. The direction of water diffusion can indicate myelin sheath damage and tissue changes. For this reason, DTI has been applied to various diseases such as Alzheimer's disease [10], autism [11], and stroke [12].

DTI has been proposed as an assessment for ON because it can measure FA and MD within visual pathways. Previous studies showed reduced axial diffusivity in optic tracts and decreased FA in optic radiations of patients with ON [13]. Other evidence demonstrated that AD decreases during acute ON and correlates with axonal loss [14]. Some authors have reported significantly decreased FA in optic radiations in patients with ON and neuromyelitis optica (NMO) [15, 16]. While these results indicate that ON patients exhibit visual pathway, few studies have evaluated whole-brain changes in ON. Here, we performed whole-brain voxel-based analyses of DTI data from patients with ON and healthy controls (HCs) and examined how these findings correlated with VEP.

Materials and methods

Subjects

Twelve patients with ON (four male, eight female) were recruited from the Ophthalmology Department of the First Affiliated Hospital of Nanchang University. The inclusion criteria for the acute ON group were: 1) acute vision loss with or without eye pain; 2) visual field abnormalities associated with nerve fiber damage; 3) patients with relative pupillary conduction block or abnormal VEP; 4) no clinical or laboratory evidence of compression, ischemic, toxic, genetic, metabolic, or invasive optic neuropathy; 5) no acute vision loss due to retinal disease, alternative eye disease, or nervous system disease; 6) no treatment with any drugs before resting-state functional MRI scanning; 7) no obvious abnormality in the brain parenchyma on head MRI; 8) no history of congenital or acquired diseases such as psychiatric disorders, hypertension, diabetes mellitus, or coronary artery disease and no drug, alcohol, or tobacco addictions; 9) no organ transplantation; and 10) moderate body shape and weight.

Twelve age-, sex-, and education-matched HCs (four male, eight female) were also recruited for this study. All HCs met the following criteria: 1) no abnormalities in visual pathways or brain parenchyma on head MRI, 2) no ocular disease and corrected visual acuity >1.0, 3) normal nervous system with no headaches and no psychiatric disease, and 4) no contraindications for MRI.

The study was authorized by the Ethics Committee of the first affiliated hospital of Nan Chang University. The study protocol and procedure were fully explained to each subject, and consent was obtained. The protocol followed the Declaration of Helsinki and conformed to the principles of medical ethics.

DTI acquisition

Each subject underwent spin echo single-shot echo planar imaging with the following parameters: repetition time/echo time = 7200/104 ms, number of excitations = 2, matrix = 128 × 128, field of view = 230 × 230 mm, slice number = 49, slice thickness = 2.5 mm, axial orientation, 64 nonlinear diffusion-weighting gradient directions with b = 1000 s/mm^2, and additional image without diffusion weighting (b = 0 s/mm^2).

Data processing

FMRIB's free software FSL (Oxford Centre for Functional MRI of the Brain, UK): (1) all diffusion-tensor images (DTI) were checked visually by experienced radiologists for apparent artifacts; (2) DTI was registered to corresponding b0 images with an offline transformation to cor-

rect eddy-current distortion; (3) binary brain masks of each participant from respective b0 images were obtained using the Brain Extract Tools (BET) functionality for brain extraction; (4) FMRIB's diffusion tools (FDT), the tensor of each voxel within the brain mask was calculated by a linear least-square fitting algorithm. (5) After diagonalization of the DTI, three eigenvalues (λ1>λ2>λ3) were obtained. Diffusion-related parameter maps involving fractional anisotropy (FA) and mean diffusivity (MD) were derived from the following equations:

$$FA = \frac{\sqrt{(\lambda_1 - \lambda_2)^2 + (\lambda_2 - \lambda_3)^2 + (\lambda_3 - \lambda_1)^2}}{\sqrt{2}\sqrt{\lambda_1^2 + \lambda_2^2 + \lambda_3^2}}$$

$$MD = \frac{\lambda_1 + \lambda_2 + \lambda_3}{3}$$

FA reflects the extent of directionality in the water molecular motion; MD reflects the average magnitude of its motion.

(6) Voxel-based analysis (VBA) of FA and MD was performed with Statistical Parametric Mapping (SPM8, http://www.fil.ion.ucl.ac.uk/spm). VBA was implemented as follows: (7) b0 images were normalized to Montreal Neurological Institute (MNI) space and resample to 2 × 2 × 2 mm voxels, then all subjects normalized b0 images were averaged. (8) The averaged b0 images were spatially smoothed by using an isotropic Gaussian filter with a full width at half maximum of 8 mm. Thus, a new template of b0 images was obtained in the MNI space. Subsequently, individual b0 images of both patients and healthy controls were registered to the new template, and corresponding transformation matrixes were also obtained. (9) Then, the FA and MD maps of each participant were normalized to MNI space using their respective transformation matrix and smoothed using an isotropic Gaussian filter with a full width at half maximum of 8 mm. (10) Finally, a paired t test was performed for smoothed FA and MD values obtained, respectively, between patients and healthy controls.

Statistical analysis

After the 2 sample t tests between patients and controls were performed, t value maps of FA and MD were obtained. The thresholds were set at P<0.01 (corrected for false discovery rate) with a minimum cluster size of 75 voxels.

Clinical data analysis

All patients underwent pattern-reversal VEP stimulation (RETLPORT electrophysiological instrument; Roland, Germany) in a dark room. Three active skin electrodes were placed on the scalp along the midline (over the inion) and on right and left lateral positions. VEP recording was performed at a 100-cm distance. All patients underwent monocular recording with the untested eye covered.

Using the stimulus mode with pattern-reversal VEP stimulation,the parameters were set as: stimulus frequency = 1.0 and 100 Hz, interphase = 500 ms, number of stimulations = 100, average screen brightness = 5 cd/m^2, spatial frequency = 50 ms/s, and contrast ratio = 90%. Amplitude and latency VEP values were studied at different angular dimensions of the stimulus (120', 60', and 15' for stimuli with small, medium, and large spatial frequencies, respectively). VEPs were characterized by a series of N75, P100, and N135 peaks, each characterized by a specific amplitude and latency.

Results

Demographics

Subject demographics are listed in **Table 1**. There were no obvious differences in weight (P = 0.741), age (P = 0.749), or height (P = 0.172) between the two groups. There was a significant difference between the ON and HC groups for best-corrected VA-Right (P<0.001).

FA and MD differences

Compared with the HC group, subjects with ON had significantly decreased FA in the left cerebellum posterior lobe, left superior temporal gyrus, left extra-nuclear1, right middle frontal gyrus, and left middle frontal gyrus (**Figure 1** [blue] and **Table 2**). Conversely, they exhibited increased FA in the right cerebellum_crus, right lentiform nucleus, bilateral anterior cingulum, left extra-nuclear2, and left precuneus (**Figure 1** [red] and **Table 2**). Patients with ON had increased MD in the left inferior temporal gyrus, left superior temporal gyrus, left hippocampus, left anterior cingulate/caudate, right superior

Table 1. Participant characteristics

	ON	HC	t	*p*-Value
Sex (M/F)	4/8	4/8	N/A	N/A
Handedness	12R	12R	N/A	N/A
Age (years)	44.08 ± 10.56	45.58 ± 11.37	-0.335	0.741
Weight (kg)	54.92 ± 7.48	59.00 ± 3.96	0.324	0.749
Height (cm)	159.25 ± 2.38	159.67 ± 6.67	-1.411	0.172
ON duration (days)	5.17 ± 1.64	N/A	N/A	N/A
Best-corrected VA - Right	0.24 ± 0.31	1.14 ± 0.24	-7.966	<0.001#
Best-corrected VA - Left	0.80 ± 0.51	1.12 ± 0.23	-2.003	0.058
Latency (ms) - Right of the VEP	114.03 ± 15.42	N/A	N/A	N/A
Amplitudes (μv)-Right of the VEP	6.14 ± 2.45	N/A	N/A	N/A
Latency (ms) - Left of the VEP	105.95 ± 4.23	N/A	N/A	N/A
Amplitudes (μv) - Left of the VEP	11.92 ± 5.95	N/A	N/A	N/A

Notes: Significant at #*P*<0.001, independent t-test. Abbreviations: HC, healthy control; N/A, not applicable; ON, optic neuritis; VA, visual acuity; VEP, visual evoked potential.

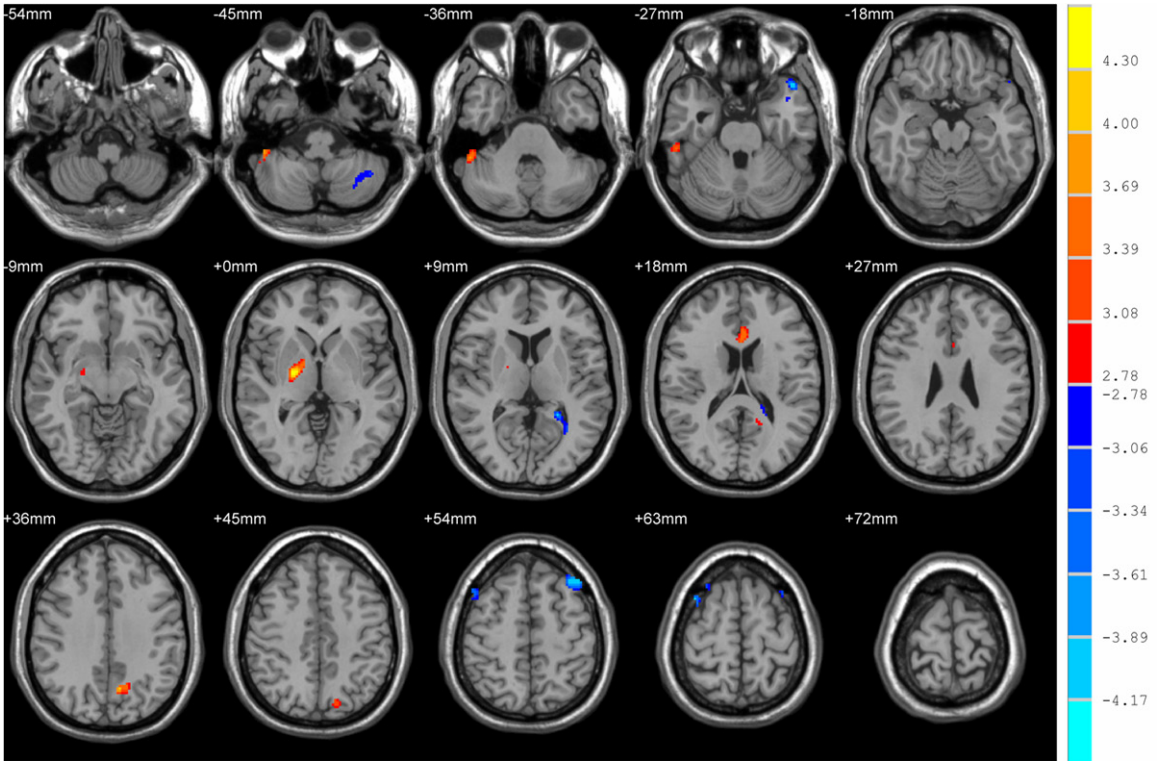

Figure 1. Overlay images demonstrating statistically significant FA alterations in ON patients and HCs. The image shows the left cerebellum posterior lobe, left superior temporal gyrus, left extra-nuclear, right middle frontal gyrus, left middle frontal gyrus, right cerebellum_crus, right lentiform nucleus, bilateralanterior cingulum, left extra-nuclear2, and left precuneus. The red and blue areas denote regions with higher and lower FA, respectively. The statistical thresholds were set at P<0.01 (corrected for false discovery rate) with a minimum cluster size of 75 voxels. Abbreviations: FA, fractional anisotropy; HC, healthy control; ON, optic neuritis.

frontal gyrus, right precentral gyrus, left inferior parietal lobule (**Figure 2** [red] and **Table 3**). The mean MD and FA values of both groups are shown in **Figure 3A** and **3B**.

Correlation analysis

The results of correlation analyses are graphically represented in **Figure 4**. In the ON group,

Table 2. Brain regions with significant between-group differences in FA

Condition	ON group and healthy control		Voxels	MNI coordinates			Peak value t-score
	Brain areas	BA		X	Y	Z	
ON<HC							
Left cerebellum posterior lobe	-		125	-38	-54	-46	-3.6151
Left superior temporal gyrus	38		98	-46	20	-24	-4.4492
Left extra-nuclear1	-		107	-24	-46	12	-4.186
Right middle frontal gyrus	6		181	42	12	62	-4.2278
Left middle frontal gyrus	8		199	-34	28	56	-4.369
ON>HC							
Right cerebellum_crus	-		170	52	-40	-40	4.4597
Right lentiform nucleus	-		223	22	-8	0	4.6043
Bilateralanterior cingulum	24		186	-2	22	22	3.9175
Left extra-nuclear2	-		90	-16	-52	24	4.0764
Left precuneus	7		133	-10	-64	36	4.0553

Notes: The statistical thresholds were set at $P<0.05$ (corrected for false discovery rate) with a minimum cluster size of 75 voxels. Abbreviations: BA, Brodmann area; FA, fractional anisotropy; HCs, healthy controls; MNI, Montreal Neurological Institute; ON, optic neuritis.

right-eye VEP latency in the ON group correlated positively with bilateral anterior cingulum FA (r = -0.583, P = 0.047) and negatively with left superior temporal gyrus FA (r = 0.653, P = 0.021). The VEP amplitude of the right eye in ON exhibited a negative correlation with left extra-nuclear2 FA (r = -0.592, P = 0.043). Left-eye VEP latency in the ON group correlated positively with MD value of the left anterior cingulate/caudate MD (r = 0.707, P = 0.010) and negatively with left inferior parietal lobule MD (r = 0.670, P = 0.017), while left-eye VEP amplitude in ON showed a negative correlation with left inferior parietal lobule MD (r = -0.684, P = 0.014).

The details are presented in **Figure 4**.

Discussion

We previously reported that the spontaneous brain-activity of patients with optic neuritis by magnetic resonance images [17-19]. The goal of our study was to evaluate FA and MD values in the whole brains of subjects with ON using DTI. We found that ON patients had significantly decreased FA in the left cerebellum posterior lobe, left superior temporal gyrus, left extra-nuclear1, right middle frontal gyrus, and left middle frontal gyrus and increased FA in the right cerebellum_crus, right lentiform nucleus, bilateral anterior cingulum, left extra-nuclear2 and left precuneus. Meanwhile, increased MD was noted in the left inferior temporal gyrus, left superior temporal gyrus, left hippocampus, left anterior cingulate/caudate, right superior frontal gyrus, right precentral gyrus, and left inferior parietal lobule. Furthermore, We observed that the changes of FA and MD values showed correlation with VEP outcomes.

The cerebellum is involved in balance and motor and is also linked to “cognitive” networks that include the prefrontal and parietal association cortices [20]. Cerebellum connections to the prefrontal lobe are involved in motor operations and eye movement control [21]. Previous studies have implicated cerebellar in autism [22], schizophrenia [23], and ataxia [24]. Redondo and colleaguesreported Purkinje axonal spheroids and Purkinje cell loss in the cerebellum of patients with MS [25]. In our previous studies have showed that significantly decreased amplitude of low-frequency fluctuation (ALFF) values in the posterior and anterior lobes of the right cerebellum and lower regional homogeneity (ReHo) in the left cerebellum in the patients with ON [18, 19]. In support of these findings, we found that patients with ON had lower FA values in the left cerebellum posterior lobe. That is to say, ON may involve tissue abnormalities in cerebellum, which may reflect dysfunction of cerebellum in ON.

The default mode network (DMN) shows greater activity when individuals are at rest [26] and plays an important role in maintaining central nervous system homeostasis [27]. DMN dysfunction has been described in multiple conditions such as schizophrenia [28], Alzheimer disease [29], and depression [30]. The DMN includes multiple brain regions including the medial prefrontal cortex, superior and inferior prefrontal cortices, anterior cingulate cortex, and orbitofrontal cortex [31]. In our recent researches have showed that ON may involve dysfunction in the default-mode network using

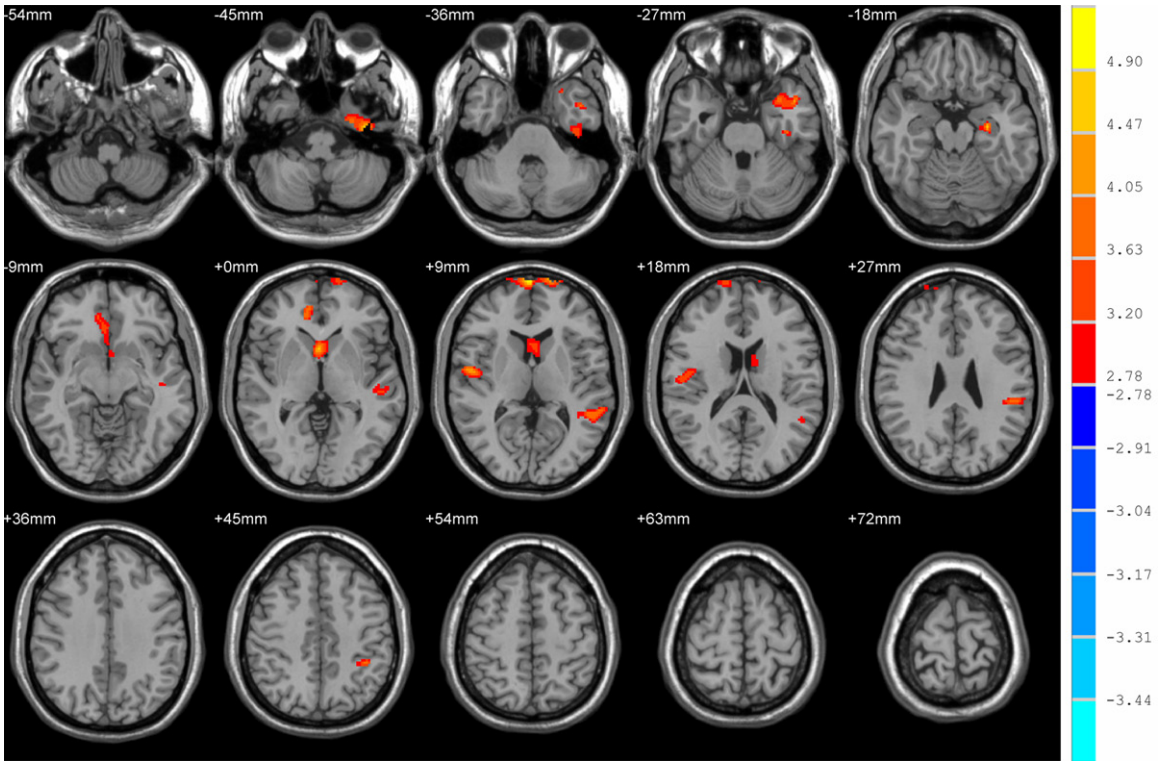

Figure 2. Overlay images demonstrating significantly greater MD in ON patients compared to HCs. The image shows the left inferior temporal gyrus, left superior temporal gyrus1, left hippocampus, left superior temporal gyrus2, left anterior cingulate/caudate, right superior frontal gyrus, left superior temporal gyrus3, right precentral gyrus, left inferior parietal lobule1, and left inferior parietal lobule2. The red and blue areas denote regions with higher and lower MD, respectively. The statistical thresholds were set at P<0.01 (corrected for false discovery rate) with a minimum cluster size of 75 voxels. Abbreviations: HC, healthy control; MD, mean diffusion; ON, optic neuritis.

Table 3. Brain regions with significant between-group differences in MD

Condition	ON group and healthy control		Voxels	MNI coordinates			Peak voxel t-score
	Brain areas	BA		X	Y	Z	
ON>HC							
Left inferior temporal gyrus		20	366	-40	-16	-42	4.6858
Left superior temporal gyrus1		21	277	-44	8	-26	4.0646
Left hippocampus			81	-28	-14	-16	4.9201
Left superior temporal gyrus2		22	96	-54	-24	-2	4.0017
Left anterior cingulate/caudate		25,32	734	2	12	0	4.4833
Right superior frontal gyrus		10	476	4	72	8	5.3195
Left superior temporal gyrus3		22	205	-50	-46	12	4.13
Right precentral gyrus		6,43,13	267	52	-6	8	4.7676
Left inferior parietal lobule1		40	113	-50	-34	26	4.2027
Left inferior parietal lobule2		40	81	-38	-42	44	4.3365

Notes: The statistical thresholds were set at *P*<0.05 (corrected for false discovery rate) with a minimum cluster size of 75 voxels.

ALFF and ReHo techniques [18, 19]. Interestingly, we found that patients with ON had lower FA in the left superior temporal gyrus and bilateral middle frontal gyrus. We also observed increased MD in the left inferior temporal gyrus, left superior temporal gyrus, left hippocampus, left anterior cingulate/caudate, and right superior frontal gyrus. Collectively, the lower FA and higher MD in these brain regions indicate that ON may lead to DMN damage. Furthermore, we found that VEP latency of the right eye in ON correlated negatively with left superior temporal gyrus FA (r = 0.653, P =

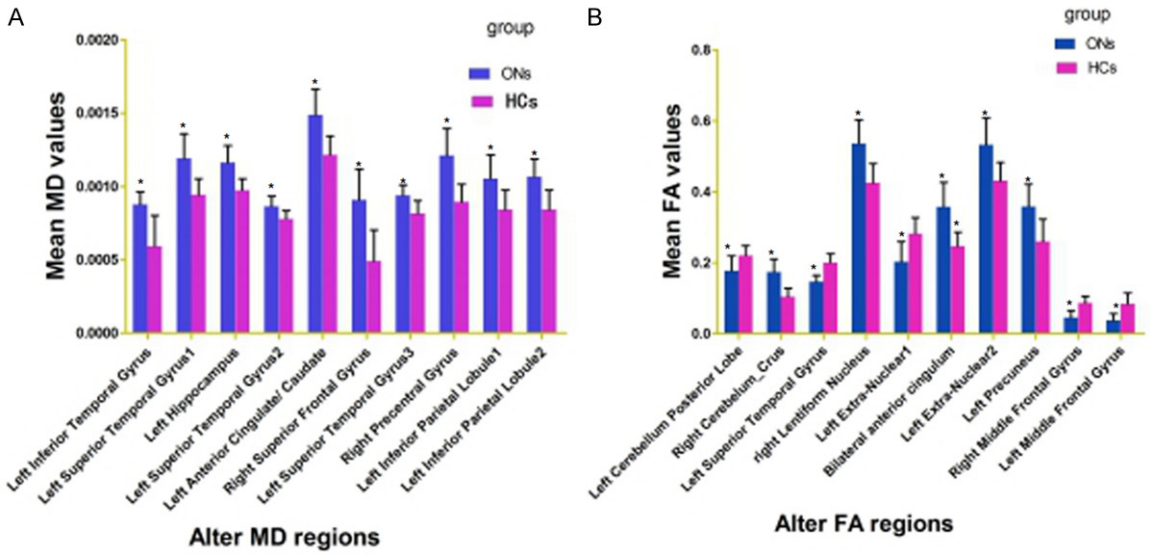

Figure 3. The mean of altered MD and FA values between the ONs and HCs. Abbreviations: MD, mean diffusion; FA, fractional anisotropy; HC, healthy control; ON, optic neuritis.

0.021). As we all know that, the prolonged VEP latency reflects the degree of optic nerve injury. We therefore conclude that decreased FA values in the left superior temporal gyrus may relate to the severity of ON.

Extra-nuclear region contains major fibers linking the striatum and frontoparietal cortex, and structural alterations in this pathway [32]. Extra-nuclear dysfunction has been described in multiple conditions such as major depressive disorder [33], schizophrenia [34] and depressive [35]. In our study, we found that decreased FA values in the extra-nuclear1 (x = -24, y = -46, z = 12), That is, the ON may lead to the dyfunction of extra-nuclear. However, we also observed that increased FA values in extra-nuclear2 (x = -16, y = -52, z = 24). The increased FA values in neighboring brain regions may reflect functional reorganization to compensate for the damaged area. Furthermore, we found that VEP amplitude of the right eye in ON showed a negative correlation with left extra-nuclear2 FA (r = -0.592, P = 0.043). The reduced VEP amplitude reflect the severity of nerve injury. We therefore come to conclusion that the increased FA values in left extra-nuclear2 may reflect the severity of ON.

Inferior parietal lobule (IPL) comprises the lateral bank of the intraparietal sulcus (IbIPS), angular gyrus (AG), and supramarginal gyrus (SMG) [36]. Meanwhile, the intraparietal sulcus is associated with the processing of visual space information [37]. In our study, we found that decreased MD values in left inferior parietal lobule in ON. We come to conclusion that the ON may lead to the dysfunction of left inferior parietal lobule. Moreover, We also observed that VEP amplitude of the left eye in ON showed negative correlation with left inferior parietal lobule2 MD (r = -0.684, P = 0.014). The reduced VEP amplitude reflected the severity of nerve damage. Therefore, the increased MD values of the left inferior parietal lobule may related to the severity of ON.

Conclusion

In summary, we found that patients with ON had abnormal brain morphology changes, which showed correlations with the VEP results in ON. These findings provide important information for the understanding of the neural mechanisms underlying ON. However, there are some limitations to our study, such as the relatively small sample size, and the lack of comparison between patients before and after treatment. In future studies we will use other techniques to explore changes in brain function in patients with ON.

Acknowledgements

This study was supported by the National Natural Science Foundation of China (81160118,

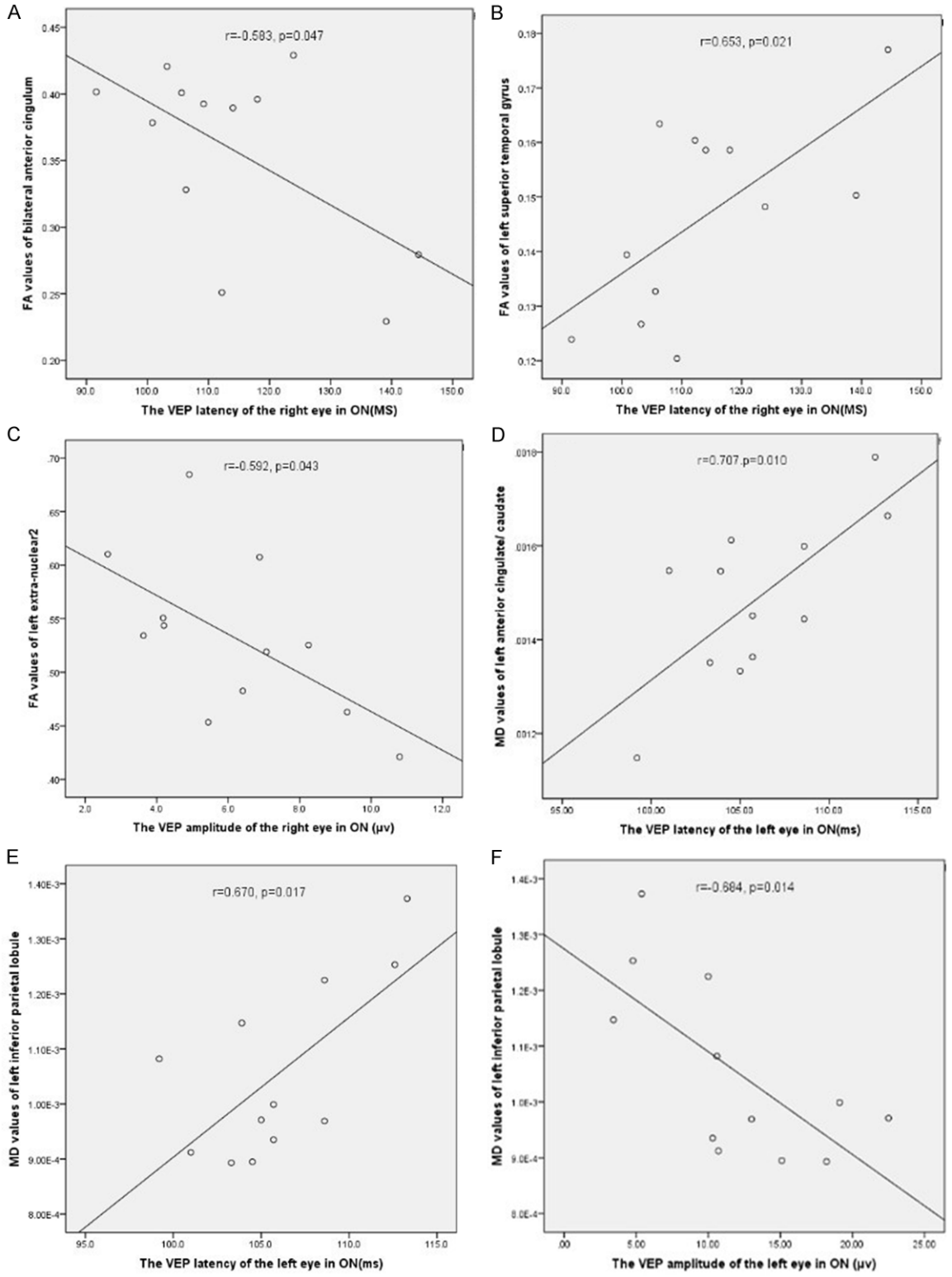

Figure 4. Correlations between the FA and MD values of the different brain regions and the VEP. Notes: The VEP latency of the right eye in ON showed a negative correlation with the FA value of the bilateral anterior cingulum (r = -0.583, P = 0.047) (A) and showed a positive correlation with the FA value of the left superior temporal gyrus (r = 0.653, P = 0.021) (B). The VEP amplitude of the right eye in ON showed a negative correlation with the FA values of the left extra-nuclear2 (r = -0.592, P = 0.043) (C). The VEP latency of the left eye in ON positively correlated with MD values of the left anterior cingulate/caudate (r = 0.707, P = 0.010) (D) and left inferior parietal lobule (r = 0.670, P = 0.017) (E). The VEP amplitude of the left eye in ON showed a negative correlation with MD values of the left

inferior parietal lobule (r = -0.684, P = 0.014) (F). Abbreviations: FA, fractional anisotropy; MD, mean diffusion; ON, optic neuritis; VEP, visual evoked potential.

81100648, 81400372 and 81660158); Clinical Medicine Research Special-purpose Foundation of China (L2012052); Jiangxi Province Voyage Project (2014022); Natural Science Key Project of Jiangxi Province (20161ACB21017); Science and Technology Platform Construction Project of Jiangxi Province (2013116); Youth Science Foundation of Jiangxi Province (2015-1BAB215016); Technology and Science Foundation of Jiangxi Province (20151BBG70223); Jiangxi Province Education Department Scientific Research Foundation (GJJ14170); Hunan Province Education Department Outstanding Youth Science Foundation (15B210); Health Development Planning Commission Science Foundation of Jiangxi Province (20155154); Scholor Project of Ganjiang River (2015).

Disclosure of conflict of interest

None.

Address correspondence to: Yi Shao, Department of Ophthalmology, The First Affiliated Hospital of Nanchang University, No 17, Yongwaizheng Street, Donghu District, Nanchang 330006, Jiangxi, People's Republic of China. Tel: +086 791-88692520; Fax: +086 791-88692520; E-mail: freebee99@163.com

References

[1] Wilhelm H, Schabet M. The Diagnosis and Treatment of Optic Neuritis. Dtsch Arztebl Int 2015; 112: 616-625; quiz 626.

[2] Hojjati SM, Zarghami A, Hojjati SA, Baes M. Optic neuritis, the most common initial presenting manifestation of multiple sclerosis in northern Iran. Caspian J Intern Med 2015; 6: 151-155.

[3] Beck RW, Cleary PA, Anderson MM Jr, Keltner JL, Shults WT, Kaufman DI, Buckley EG, Corbett JJ, Kupersmith MJ, Miller NR, et al. A randomized, controlled trial of corticosteroids in the treatment of acute optic neuritis. The Optic Neuritis Study Group. N Engl J Med 1992; 326: 581-588.

[4] Hickman SJ, Kapoor R, Jones SJ, Altmann DR, Plant GT, Miller DH. Corticosteroids do not prevent optic nerve atrophy following optic neuritis. J Neurol Neurosurg Psychiatry 2003; 74: 1139-1141.

[5] Klistorner A, Arvind H, Nguyen T, Garrick R, Paine M, Graham S, O'Day J, Grigg J, Billson F, Yiannikas C. Axonal loss and myelin in early ON loss in postacute optic neuritis. Ann Neurol 2008; 64: 325-331.

[6] Alshowaeir D, Yannikas C, Garrick R, Van Der Walt A, Graham SL, Fraser C, Klistorner A. Multifocal VEP assessment of optic neuritis evolution. Clin Neurophysiol 2015; 126: 1617-1623.

[7] Klistorner A, Arvind H, Garrick R, Graham SL, Paine M, Yiannikas C. Interrelationship of optical coherence tomography and multifocal visual-evoked potentials after optic neuritis. Invest Ophthalmol Vis Sci 2010; 51: 2770-2777.

[8] Beaulieu C. The basis of anisotropic water diffusion in the nervous system - a technical review. NMR Biomed 2002; 15: 435-455.

[9] Pierpaoli C, Basser PJ. Toward a quantitative assessment of diffusion anisotropy. Magn Reson Med 1996; 36: 893-906.

[10] Hořínek D, Štěpán-Buksakowska I, Szabó N, Erickson BJ, Tóth E, Šulc V, Beneš V, Vrána J, Hort J, Nimsky C, Mohapl M, Roček M, Vécsei L, Kincses ZT. Difference in white matter microstructure in differential diagnosis of normal pressure hydrocephalus and Alzheimer's disease. Clin Neurol Neurosurg 2016; 140: 52-59.

[11] Jou RJ, Jackowski AP, Papademetris X, Rajeevan N, Staib LH, Volkmar FR. Diffusion tensor imaging in autism spectrum disorders: preliminary evidence of abnormal neural connectivity. Aust N Z J Psychiatry 2011; 45: 153-162.

[12] Chaudhary N, Pandey AS, Gemmete JJ, Hua Y, Huang Y, Gu Y, Xi G. Diffusion tensor imaging in hemorrhagic stroke. Exp Neurol 2015; 272: 88-96.

[13] Raz N, Bick AS, Ben-Hur T, Levin N. Focal demyelinative damage and neighboring white matter integrity: an optic neuritis study. Mult Scler 2015; 21: 562-571.

[14] van der Walt A, Kolbe SC, Wang YE, Klistorner A, Shuey N, Ahmadi G, Paine M, Marriott M, Mitchell P, Egan GF, Butzkueven H, Kilpatrick TJ. Optic nerve diffusion tensor imaging after acute optic neuritis predicts axonal and visual outcomes. PLoS One 2013; 8: e83825.

[15] Kolbe S, Bajraszewski C, Chapman C, Nguyen T, Mitchell P, Paine M, Butzkueven H, Johnston L, Kilpatrick T, Egan G. Diffusion tensor imaging of the optic radiations after optic neuritis. Hum Brain Mapp 2012; 33: 2047-2061.

[16] Kimura MC, Doring TM, Rueda FC, Tukamoto G, Gasparetto E. In vivo assessment of white matter damage in neuromyelitis optica: a diffusion tensor and diffusion kurtosis MR imaging study. J Neurol Sci 2014; 345: 172-175.
[17] Huang X, Zhang Q, Hu PH, Zhong YL, Zhang Y, Wei R, Xu TT, Shao Y; Oculopathy fMRI Study Group. White and Gray Matter Volume Changes and Correlation with Visual Evoked Potential in Patients with Optic Neuritis: A Voxel-Based Morphometry Study. Med Sci Monit 2016; 22: 1115-23.
[18] Huang X, Cai FQ, Hu PH, Zhong YL, Zhang Y, Wei R, Pei CG, Zhou FQ, Shao Y. Disturbed spontaneous brain-activity pattern in patients with optic neuritis using amplitude of low-frequency fluctuation: a functional magnetic resonance imaging study. Neuropsychiatr Dis Treat 2015; 11: 3075-83.
[19] Shao Y, Cai FQ, Zhong YL, Huang X, Zhang Y, Hu PH, Pei CG, Zhou FQ, Zeng XJ. Altered intrinsic regional spontaneous brain activity in patients with optic neuritis: a resting-state functional magnetic resonance imaging study. Neuropsychiatr Dis Treat 2015; 11: 3065-73.
[20] Stoodley CJ. The cerebellum and cognition: evidence from functional imaging studies. Cerebellum 2012; 11; 352-365.
[21] Doron KW, Funk CM, Glickstein M. Fronto-cerebellar circuits and eye movement control: a diffusion imaging tractography study of human cortico-pontine projections. Brain Res 2010; 1307: 63-71.
[22] Mosconi MW, Wang Z, Schmitt LM, Tsai P, Sweeney JA. The role of cerebellar circuitry alterations in the pathophysiology of autism spectrum disorders. Front Neurosci 2015; 9: 296.
[23] Bernard JA, Mittal VA. Dysfunctional Activation of the Cerebellum in Schizophrenia: A Functional Neuroimaging Meta-Analysis. Clin Psychol Sci 2015; 3: 545-566.
[24] Kim WS, Jung SH, Oh MK, Min YS, Lim JY, Paik NJ. Effect of repetitive transcranial magnetic stimulation over the cerebellum on patients with ataxia after posterior circulation stroke: A pilot study. J Rehabil Med 2014; 46: 418-423.
[25] Redondo J, Kemp K, Hares K, Rice C, Scolding N, Wilkins A. Purkinje Cell Pathology and Loss in Multiple Sclerosis Cerebellum. Brain Pathol 2015; 25: 692-700.
[26] Raichle ME, MacLeod AM, Snyder AZ, Powers WJ, Gusnard DA, Shulman GL. A default mode of brain function. Proc Natl Acad Sci U S A 2001; 98: 676-682.
[27] Buckner RL, Andrews-Hanna JR, Schacter DL. The brain's default network: anatomy, function, and relevance to disease. Ann N Y Acad Sci 2008; 1124: 1-38.
[28] Pankow A, Deserno L, Walter M, Fydrich T, Bermpohl F, Schlagenhauf F, Heinz A. Reduced default mode network connectivity in schizophrenia patients. Schizophr Res 2015; 165: 90-93.
[29] Chang YT, Huang CW, Chang YH, Chen NC, Lin KJ, Yan TC, Chang WN, Chen SF, Lui CC, Lin PH, Chang CC. Amyloid burden in the hippocampus and default mode network: relationships with gray matter volume and cognitive performance in mild stage Alzheimer disease. Medicine (Baltimore) 2015; 94: e763.
[30] Shi H, Wang X, Yi J, Zhu X, Zhang X, Yang J, Yao S. Default mode network alterations during implicit emotional faces processing in first-episode, treatment-naive major depression patients. Front Psychol 2015; 6: 1198.
[31] Wu J, Dong D, Jackson T, Wang Y, Huang J, Chen H. The Neural Correlates of Optimistic and Depressive Tendencies of Self-Evaluations and Resting-State Default Mode Network. Front Hum Neurosci 2015; 9: 618.
[32] Su L, Cai Y, Xu Y, Dutt A, Shi S, Bramon E. Cerebral metabolism in major depressive disorder: a voxel-based meta-analysis of positron emission tomography studies. BMC Psychiatry 2014; 14: 321.
[33] Lei W, Li N, Deng W, Li M, Huang C, Ma X, Wang Q, Guo W, Li Y, Jiang L, Zhou Y, Hu X, McAlonan GM, Li T. White matter alterations in first episode treatment-naive patients with deficit schizophrenia: a combined VBM and DTI study. Sci Rep 2015; 5: 12994.
[34] Peng H, Ning Y, Zhang Y, Yang H, Zhang L, He Z, Li Z, Wang L, Lu S, Zhou J, Zhang Z, Li L. White-matter density abnormalities in depressive patients with and without childhood neglect: a voxel-based morphometry (VBM) analysis. Neurosci Lett 2013; 550: 23-28.
[35] Kring AM, Barch DM. The motivation and pleasure dimension of negative symptoms: neural substrates and behavioral outputs. Eur Neuropsychopharmacol 2014; 24: 725-736.
[36] Zhang S, Li CS. Functional clustering of the human inferior parietal lobule by whole-brain connectivity mapping of resting-state functional magnetic resonance imaging signals. Brain Connect 2014; 4: 53-69.
[37] Egner T, Monti JM, Trittschuh EH, Wieneke CA, Hirsch J, Mesulam MM. Neural integration of top-down spatial and feature-based information in visual search. J Neurosci 2008; 28: 6141-6151.